Magic Numbers in Formic Acid Water Clusters Revealed by VUV Photoionization Mass Spectrometry and Density Functional Calculations

Amit Daniely,[†] Nevo Levy,[†] Omri Sheffer,[†] Anna Wannenmacher,[‡] Edwin Joseph,[†] Oleg Kostko,[‡] Musahid Ahmed,[‡] and Tamar Stein[*,†]

[†]*The Fritz Haber Center for Molecular Dynamics, Department of Chemistry, The Hebrew University*

[‡]*Chemical Sciences Division, Lawrence Berkeley National Laboratory, Berkeley, California 94720*

E-mail: tamar.stein@mail.huji.ac.il

Abstract

The interaction between formic acid (FA) and water (W) holds significant importance in various chemical processes. Our study combines vacuum-ultraviolet photoionization mass spectrometry with density functional calculations to investigate formic acid water clusters generated in supersonic molecular beams. The mass spectra obtained reveal the formation of protonated clusters as the major product. Magic numbers observed in the mass spectra include $FA_1W_5H^+$, $FA_2W_4H^+$, $FA_3W_3H^+$, $FA_4W_2H^+$, $FA_5W_1H^+$ and $FA_6W_2H^+$ clusters. Interestingly, adding water to these magic number clusters leads to reduced stability. Our calculations shed light on the potentially stable structures, highlighting cyclic arrangements with molecules enclosed within the ring as the most stable structures, and demonstrate a decrease in the stability upon the addition of a water molecule. Comparing experimental appearance energies with calculated ionization energies suggests that the observed clusters are likely a result of fragmentation of larger clusters.

Introduction

Formic acid (FA), HCOOH, is the smallest carboxylic acid with pivotal roles in atmospheric,[1] prebiotic[2,3] and catalytic chemistry.[4,5] Its interactions with water, both in the rarefied atmospheres of earth and on catalytic surfaces, can have profound effects on the resulting chemistry. FA is also important in astrochemistry, and was recently found to be present in interstellar ices,[6] and can take part in the formation of amino acids such as glycine.[7,8] To date there have been many studies, both experimental and theoretical, including quantum chemical calculations,[4,9–24] aiming at understanding the mechanisms at play. Early work employed mass spectrometry to probe the thermodynamics and structure of FA clusters employing collision-induced ionization,[9,16,25,26] electron impact[27,28] and VUV photoionization.[29] Very recently an electron impact ionization study of negatively and positively charged FA water clusters was reported coupled to theoretical calculations of the stability of neutral, cationic and anionic clusters.[30] While some clusters were identified to be more stable, particularly in cyclic geometries, no systematic attempt was made to correlate the stability of these clusters with that of the appearance of magic numbers in the mass spectra as the emphasis of the study was to identify the distribution of neutral FA water clusters. The consensus that emerged, is that for FA clusters with water, open chain structures with water bound to the end are favored for $n<4$, while the hydronium ion acts as a nucleation site beyond $n = 4$, and the open chains tend to take cyclic structures. FA pentamer with hydronium ion has been implicated as a magic number as observed in different mass spectrometry experiments,[27,28] and theoretical calculations suggest that the hydronium is located at the center of a ring composed of five FA molecules. Beyond stabilizing certain magic structures, water clusters can also play a catalytic role in the dehydration and decarboxylation of FA,[4,5,31] presumably via cis-trans isomerization dynamics, where the cis isomer leads to decarboxylation and the trans isomer follows the dehydration pathway.

However, the question of ionization pathways, particularly proton transfer between FA clusters, and its interaction with water remains unresolved and recently there have been several experimental and theoretical studies which have attempted to shed light on this problem. Electron ionization of FA clusters embedded in helium nanodroplets showed both anionic and protonated FA clusters.[32] The authors discussed their results in the context of the stability of the ions in the cold environment of helium nanodroplets and suggested that mass spectral distributions could have a very sensitive dependence on source and ionization conditions. It was revealed that beyond protonated FA clusters, there are other fragmentation channels which could lead to the formation of new moieties complexed with water. Tachikawa et al.[23] performed direct *ab-initio* molecular dynamics (AIMD) and suggested that the FA dimer cation could form a complex, where the carbonyl oxygen atom was bound symmetrically leading to the formation of a face-to-face complex. However, with increasing temperature, a proton transferred $H^+(HCOOH)$-HCO_2 radical cation would be dominant with a 78% formation probability at room temperature, and absent at 0 K. Very recently, Sutton et al., using ultrafast time-resolved pump-probe mass spectrometry, monitored the proton transfer pathway following Rydberg state excitation for a series of FA clusters.[33] A contact ion-pair mechanism was shown to be operational leading finally to a protonated FA cluster and the $HCOO^-$ anion. This pathway was absent in the FA dimer, a pathway purported to be operational upon VUV excitation, but whose efficiency increased with the number of FA clusters bound in the system. Recently, intra-cluster charge migration upon hydration of protonated FA was studied using both cold ion vibrational spectroscopy coupled with path integral *ab-initio* molecular dynamics simulations.[34] The authors suggested that FA could be considered formally protonated when being hydrated by a maximum of three water molecules. Beyond that, as the water cluster number increases, the proton transfer occurs and the excess proton is accommodated by the extended water network and the neutral FA. There has also been a study recently where photoionization and electron impact ionization of FA and methanol co-deposited together on cold argon clusters led to interesting mixed cluster proton transfer reactions.[35]

In this work, we perform a systematic study combining theory and experiment in unravelling the photoionization dynamics of mixed FA water clusters. We present a synchrotron-based VUV photoionization[36] study of the mixed clusters formed in a supersonic expansion coupled with electronic structure calculations, where both E and Z conformers of FA are taken into account, to understand the photoionization dynamics. The employed methodology includes intensity measurements of various masses at variable photon energies, the appearance energies of various fragments, and an interpretation of their stability guided by theoretical calculations. This approach, previously used in studying proton transfer in acetaldehyde water clusters[37] and naphthalene water clusters,[38] also contributed to identifying magic numbers in water clusters beyond the traditional "21"[39] and the identification of the hydrogen bond networks in diol[40] and polyol water clusters.[41]

Mass spectra results demonstrate that upon ionization of mixed FA-water clusters, the resulting clusters are protonated. The stability of magic numbers of different FA-water clusters was observed in the mass spectra, specifically for clusters: $FA_1W_5H^+$, $FA_2W_4H^+$, $FA_3W_3H^+$, $FA_4W_2H^+$, $FA_5W_1H^+$, $FA_6W_2H^+$. Additionally, we observe that adding water to the magic number structures results in the diminishing of their stability. The trends are explained in terms of the normalised binding energy (nBE) of each of the structures, showing a larger nBE for the more stable structures. The stable structures are those forming rings with molecules enclosed inside them. Experimental appearance energies (AE) are only slightly influenced by cluster size, whether in terms of the number of FA or water molecules. Comparing the experimental values to calculated ionization energies of different cluster sizes suggests that the clusters observed in the experiment likely result from fragmentation of larger clusters.

Methods

Experimental Details

The experiment was performed with a reflectron time-of-flight mass spectrometer containing a continuous supersonic expansion molecular beam source connected to a 3-meter vacuum monochromator and attached to the Chemical Dynamics Beamline (9.0.2) located at the Advanced Light Source. For a detailed description of the instruments, refer to previous studies.[36,42,43] The FA is placed in a bubbler at room temperature (vapor pressure of 30 torr at 20°C), and entrained in argon (460 torr) carrier gas leading to a 6.5 percent molecular beam of FA in argon. To generate a FA water mixture, a second bubbler is introduced in-line before the FA bubbler containing water at room temperature (20°C) leading to a vapor pressure of 17.5 torr. This method of introduction is different from earlier reports[29,30,32] where FA and water were mixed in the same reservoir. The gas mixture passes through a 100 μm nozzle source and supersonically expands into a vacuum chamber, yielding the desired FA water molecular beam. This beam is extracted through a skimmer into a deferentially pumped interaction region where the clusters are exposed to and ionized by VUV synchrotron radiation. The ionized species are then detected using a reflectron time-of-flight mass spectrometer. Mass spectra are recorded at photon energies between 9.5 and 14.5 eV every 50 meV. Photoionization efficiency curves, which show ion count versus photon energy (in eV), of the ionized clusters are obtained by integrating over the peaks in the mass spectrum at each photon energy after being normalized by the photon flux.

Computational Details

All structural optimizations were performed using density functional theory (DFT) with the Q-Chem 5.4 software package.[44] The clusters were optimized using the ωB97X-V functional[45] with an aug-cc-pVDZ[46] basis set and the obtained structures confirmed as minimum points on the PES via frequency calculations. For more accurate energies, we performed singlepoint calculations of all optimal structures using ωB97X-V functional with an aug-cc-pVTZ basis set. The binding energies (BE) of the protonated structures were calculated according to the following equation (E represents energy, N represents number of molecules)

$$BE_{protonated\,cluster} = E_{cluster} - N_{FA} \cdot E_{FA} - N_W \cdot E_W - N_{FAH^+} \cdot E_{FAH^+} - N_{WH^+} \cdot E_{WH^+} \quad (1)$$

Normalized BE (nBE) are calculated according to the following equation

$$nBE = \frac{BE}{N_{total}} \quad (2)$$

In order to calculate the ionization energy (IE) of different conformers for different cluster sizes, we used the Packmol package[47] to build different possible structures. For FA_nW_m clusters we started by building $n + m$ structures and added structures for the small clusters. The total number of sampled structures for each cluster is given in the SI in table S1. The structures were then optimized using B3LYP[48]/6-31+G* to obtain realistic distances. IEs were evaluated from the optimized structures using ωB97X-V/aug-cc-pVTZ.

Results and discussion

Mass Spectra

The mass spectra of FA water clusters obtained with a photon energy of 12.5 eV is shown in Figure 1. A series of protonated FA clusters with up to 7 FA molecules are observed, along with clusters of these protonated FA moieties and water molecules (series indicated in figure 1 by the colored dots). There are also fragments (m/z 17, 28, 29, 30, 44, and 45) below the mass of the FA monomer (m/z 46), notably OH^+, CO^+, HCO^+ or COH^+, $HCOH^+$, $CO_2{}^+$, and $HCOO^+$, however they are not the subject of discussion in this work. While the FA monomer and a vastly diminished FA dimer (m/z 92) are observed in the mass spectra, no other non protonated clusters of FA are detected. The other mass peak that is observed with reasonable intensity is the mass at m/z 91 which is assigned to $(HCOOH)_2H^+$ - H_2. The distribution of the FA water clusters is displayed as colored dots and the lines connecting them show a dramatic departure from a smooth trend. For FA_1H^+ (m/z 47), the distribution decays smoothly till $FA_1W_5H^+$ (m/z 137), and then there is a sharp drop in intensity. For FA_2H^+ (m/z 93), this drop occurs after $FA_2W_4H^+$ (m/z 169), and for FA_3H^+ (m/z 139) the drop is after $FA_3W_3H^+$ (m/z 193). For FA_4H^+ (m/z 185), the intensity drops slightly with the addition of one water, $FA_4W_2H^+$ (m/z 221) is enhanced, and then there is a sharp drop. In the case of FA_5H^+ (m/z 231), the results are dramatic, as one observed a rise in signal with addition of one water to $FA_5W_1H^+$ (m/z 249), and then a drop in intensity. Finally, while there is almost no signal for FA_6H^+ (m/z 277), there is an increase in signal for addition of one water to form $FA_6W_1H^+$ (m/z 295), and an increase in signal when two waters are added leading to the formation of $FA_6W_2H^+$ (m/z 313) , and then a smooth drop with addition of further waters to the cluster.

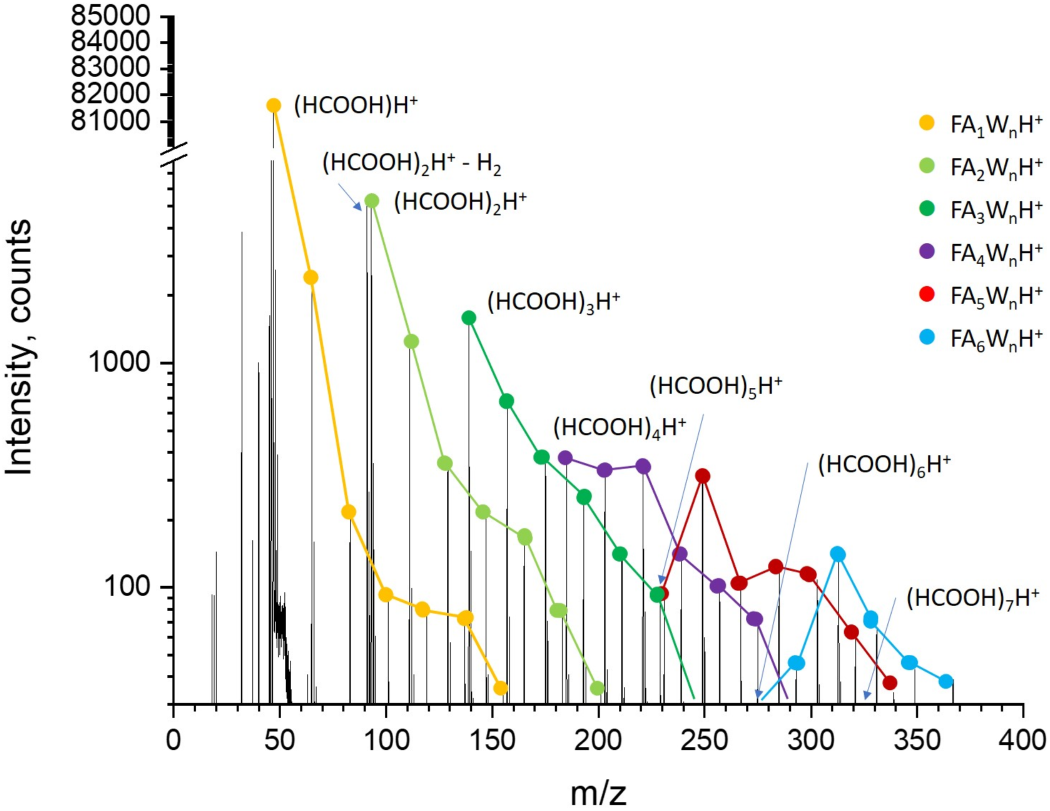

Figure 1: Mass spectrum, taken with a photon energy of 12.5 eV, showing formic acid water clusters.

This distribution occurs due to the high stability of certain cluster sizes. This is true for the following cluster sizes: $FA_1W_5H^+$, $FA_2W_4H^+$, $FA_3W_3H^+$, $FA_4W_2H^+$, $FA_5W_1H^+$, $FA_6W_2H^+$. Previously the stability of $FA_5W_1H^+$ and $FA_6W_2H^+$ formed upon electron impact ionization in supercooled helium droplets has been commented upon.[32] In that work, earlier experiments[29] which showed $FA_5W_1H^+$ and $FA_6W_2H^+$ as particularly stable were also discussed. Our results support this stability finding and additionally find that clusters containing one water more than the stable cluster ($FA_1W_6H^+$, $FA_2W_5H^+$, $FA_3W_4H^+$, $FA_4W_3H^+$, $FA_5W_2H^+$) have diminished stability. The recent work of Li et al.[30] and earlier theoretical work cited therein and in the introduction suggest that the stability of these clusters arises from their cyclic structures. Indeed, Li et al. observe very similar mass spectral distributions in a 98 percent v/v FA water beam upon electron impact ionization at 70 eV. As the water content of their mixtures was increased, the discontinuity (magic numbers) disappeared leading to smooth distributions. Hence it is clear that one needs to work within water-poor regimes to be able to generate these magic number distributions. In the next section, we will describe theoretical calculations undertaken to explain the stability of these cyclic clusters.

Photoionization Efficiency (PIE) Curves and Appearance Energies (AE)

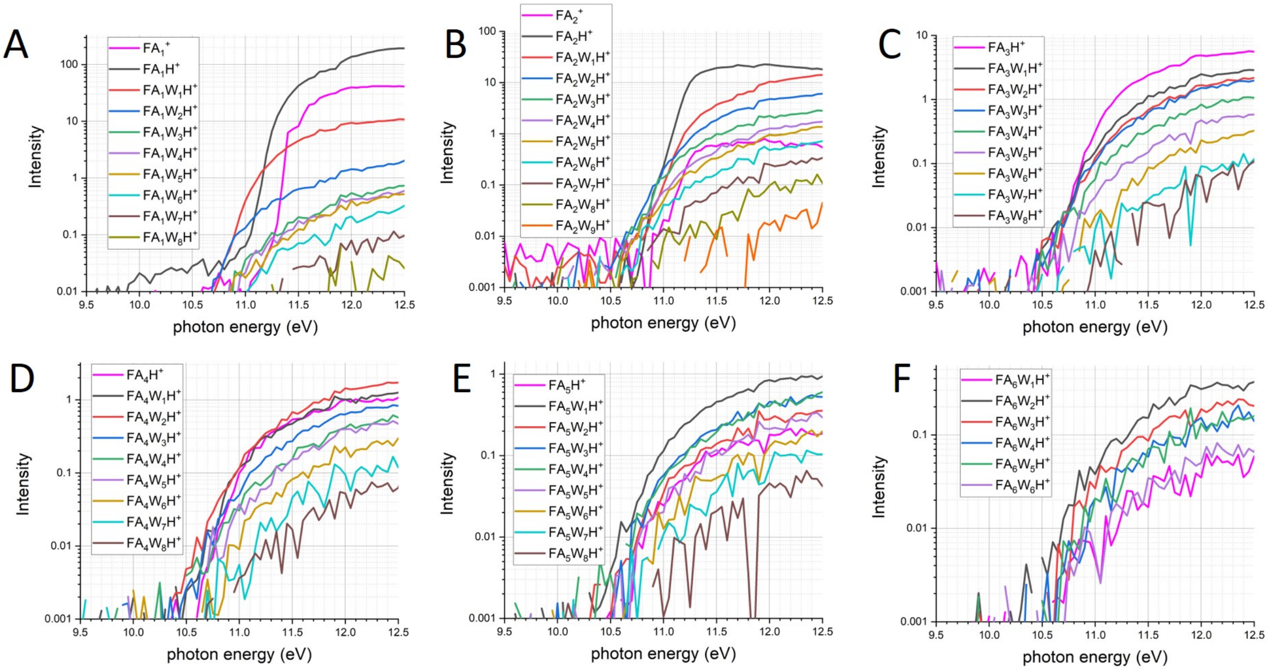

Figure 2: Photoionization Efficiency Curves in log scale for formic acid water clusters. (A) $FA_1W_nH^+$, (B) $FA_2W_nH^+$ (C) $FA_3W_nH^+$ (D) $FA_4W_nH^+$ (E) $FA_5W_nH^+$ (F) $FA_6W_nH^+$. The intensities are observed counts, providing a direct measure of absolute and relative populations of clusters in the beam.

Figure 2, shows the photoionization efficiency (PIE) curves for a series of FA water clusters extracted from the mass spectral measurements. The PIE's provide a direct visualization of the population of the clusters in the beam and allow us to extract appearance energies (AE) which are matched to calculated ionization energies as described in a subsequent section. In this work, the AE is defined as the amount of energy needed to ionize and potentially fragment the gas phase molecule or cluster. The AE value is determined via visual identification of the first major rise of the PIE curve above the baseline, as has been done previously.[49] These AE's are reported in detail in table 1 with most AE's in the 10.5 eV range. The PIE's for fragments with masses below that of FA are reported in the SI in figure S1, however, their appearance energies are reported in table 1 for completeness.

The stability of the magic number clusters identified via mass spectrometry does not change dramatically with an increase in photon energy. This is very clear when one examines Figure 2 D, E and F, where the $FA_4W_2H^+$, $FA_5W_1H^+$, and $FA_6W_2H^+$ PIE's are the largest signals and rise to the top of the graph and vary smoothly over the photon energies. For $FA_1W_5H^+$, $FA_2W_4H^+$ and $FA_3W_3H^+$ shown in Figure 2 A, B and C, the PIE's do not rise to the top, however one can discern the discontinuities, by seeing the lowering of the PIE intensities of the next cluster with one added water. The stability of these magic number clusters has been better understood through theoretical calculations of binding energies as discussed in the next section.

Table 1: Appearance energies for clusters from molecular beams with FA and water. All AEs are reported in eV. For AE fragments and clusters with n less than 4, the error in AE is ± 0.1, while for clusters with n greater than 4, the error is larger than this due to low signal-to-noise. A - either indicates a lack of observed cluster or very low signal-to-noise for that PIE curve.

Cluster	n = 0	n = 1	n = 2	n = 3	n = 4	n = 5	n = 6	n = 7	n = 8
OH^+	10.5	-	-	-	-	-	-	-	-
CO^+	11	-	-	-	-	-	-	-	-
HCO^+ or COH^+	12.1	-	-	-	-	-	-	-	-
$HCOH^+$	12.2	-	-	-	-	-	-	-	-
CO_2^+	13.6	-	-	-	-	-	-	-	-
$HCOO^+$ or $COOH^+$	12.1	-	-	-	-	-	-	-	-
FA^+	11.0	-	-	-	-	-	-	-	-
$FA_1W_nH^+$	10.6	10.5	10.5	10.5	10.5	10.8	10.8	10.7	-
FA_2^+	10.8	-	-	-	-	-	-	-	-
$FA_2W_nH^+$	10.5	10.4	10.4	10.5	10.5	10.5	10.5	10.7	10.8
$FA_3W_nH^+$	10.6	10.4	10.4	10.4	10.4	10.5	10.7	10.7	10.8
$FA_4W_nH^+$	10.6	10.4	10.3	10.3	10.4	10.6	10.6	10.6	10.6
$FA_5W_nH^+$	10.6	10.4	10.5	10.5	10.6	10.5	10.6	10.6	10.6
$FA_6W_nH^+$	-	10.5	10.4	10.5	10.4	10.5	10.6	-	-

Trends in mixed Formic Acid Water Clusters

Stability of Magic Numbers

The experimental mass spectra (Figure 1) demonstrate magic numbers for certain clusters, with diminishing stability after adding additional water molecules. We have studied various structures of $FA_4W_2H^+$, $FA_5W_1H^+$, $FA_6W_2H^+$ clusters, and the stability when adding or removing one water molecule. Here we calculate the stability in terms of how strong the cluster is bound using the nBE. As the Z conformer is lower in energy (by 4.3 kcal/mol), the structures composed of Z conformers are lower in terms of relative energy (RE), however, similar structures containing either all Z or all E conformers are usually close in the value of the nBE. Figure 3 shows the nBE of different conformers for each structure, and the structure corresponding to the highest nBE. The different structures are shown in the SI in Figures S3-S11. In agreement with the literature,[30] the most stable structures are the cyclic ones.

For the case of $FA_4W_1H^+$, the most stable structure is a cyclic structure containing only Z conformers of FA and a hydronium ion at the center. The nBE value is -19.7 kcal/mol. A cyclic isomer with E conformers of FA and a hydronium ion in the middle is also very stable with a nBE of -19.4 kcal/mol as shown in Figure S3 in the SI along with additional possible structures. Adding a water molecule, namely, $FA_4W_2H^+$, also forms a stable cyclic structure, with the most stable structure being a cyclic structure containing E conformers and one water molecule, with a hydronium ion in the middle as shown in Figure 3. The nBE is -19.6 kcal/mol, similar to the case of $FA_4W_1H^+$, in agreement with experimental results. A similar structure with Z conformers is also very stable with nBE value of -19.5 kcal/mol as shown in Figure S4 in the SI. The addition of one more water molecule, namely $FA_4W_3H^+$ cluster, results in a decrease of the stability reflected by a lower nBE value of -18.6 kcal/mol, again in agreement with experimental results that demonstrate diminished stability in structures following the magic number. The additional water molecule perturbed the formation of a stable cyclic structure with a hydronium ion in the middle, as shown in the Figure.

The next series is of magic number $FA_5W_1H^+$. With the abstraction of one water molecule, namely in cluster $FA_5W_0H^+$, the most stable structure is a cyclic structure containing three E conformers and one Z conformer (in addition to a protonated FA) with nBE of -18.9 kcal/mol. An additional stable structure composed of a cyclic structure of three E conformers and a protonated FA, with an additional E conformer external to the ring with nBE of -18.7 kcal/mol is shown in Figure S6 in the SI. For the most stable structure of $FA_5W_1H^+$, we see a significant increase in the BE, with nBE of -20.8 kcal/mol for a cyclic structure containing all E conformers and a hydronium ion in the middle. Additional stable structure with Z conformers is also very stable (nBE value of -20.1 kcal/mol) shown in Figure S7 in the SI. In $FA_5W_2H^+$ cluster, the additional water molecule can not be located inside the cyclic structure and placed above as shown in Figure 3, which results in a significant decrease in nBE (-18.7). The results are in line with the experimental mass spectra where

$FA_5W_1H^+$ has a large peak, followed by a drastic decrease.

The next series we have studied is $FA_6W_2H^+$. For $FA_6W_1H^+$, the most stable structure is again a cyclic structure of E conformers with hydronium in the middle (nBE of -19.8 kcal/mol) followed by a cyclic structure of five E conformers, with additional E conformer external to the ring, here as well, the hydronium ion is found in the middle (nBE of -19.6 kcal/mol) as shown in Figure S9. For $FA_6W_2H^+$, the most stable structure again demonstrates high stability with nBE of -20.1 kcal/mol. The structure contains a large cyclic structure with six E conformers, where a hydronium ion and a water molecule are placed in the middle of the ring above the ring plane. If the water molecule and the hydronium ion are in the molecular plane the ring opens, resulting in structure (j) as shown in Figure S10 of the SI with nBE of -19.2 kcal/mol. When the ring is composed of six Z conformers, the water and hydronium are in the middle of the ring: one above the ring plane and one below it, as shown in structure (n) in Figure S10, the corresponding nBE value is -18.7 kcal/mol.

The addition of water molecule in $FA_6W_3H^+$ results (for the most stable structure) in a structure similar to the stable structure of $FA_6W_2H^+$ cluster, with an addition of water molecule above the ring which results in decreased stability (nBE value of -18.8 kcal/mol). Including the water in the ring (as shown in Figure S11 structure (l) in the SI), results in nBE value of -18.6 kcal/mol.

The nBE trends reported here are inline with experimental trends observed in the MS. While we have not calculated the energies for $FA_3W_3H^+$, and $FA_2W_4H^+$, a recent report using a similar level of theory do report the cyclic structures as having the most stability.[30] This further supports the conclusion that indeed the mass spectrometry of VUV photoionized FA water clusters reveal the most stable "magic" numbers for the aforementioned clusters.

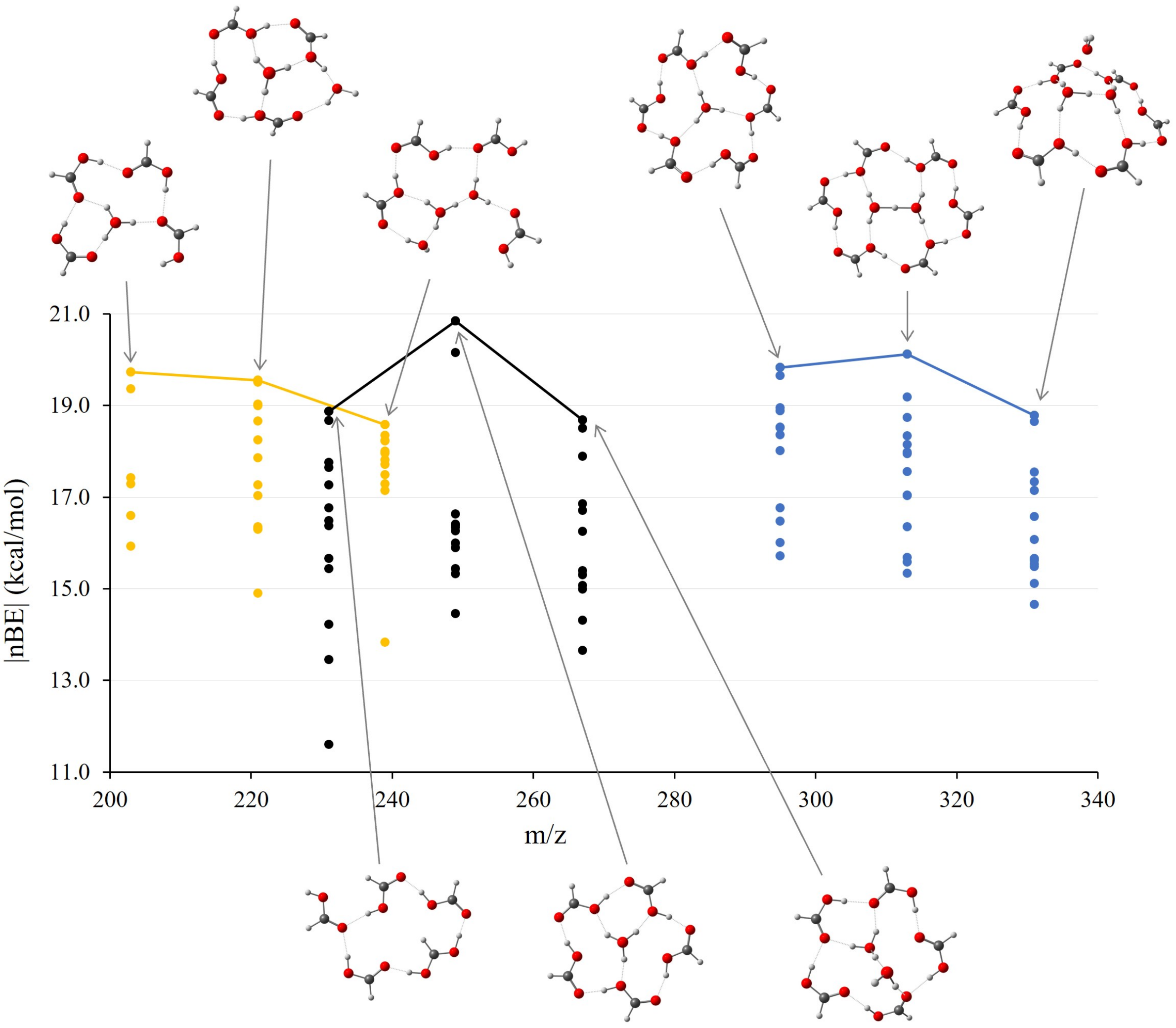

Figure 3: nBE (shown in absolute value) of various structures for each magic number cluster, and for structures with addition and removal of water molecules. Each colour represents trends of the stability of the magic number with the addition and removal of a water molecule. Yellow - $FA_4W_2H^+$, black - $FA_5W_1H^+$, blue - $FA_6W_2H^+$.

Calculated IE

To calculate the IEs of the different clusters, we generated random clusters of the Z conformer at different sizes and then optimized them using B3LYP/6-31+G* to obtain more realistic distances. IEs of the obtained conformers were calculated using ωB97X-V/aug-cc-pVTZ. Figure 4 panel (A) shows the obtained IE of the different sampled structures of FA-water clusters, the experimental value of 10.5 eV is marked with a dashed line. As can be seen from the Figure, there is a general downward trend in the IE as the cluster mass increases and small clusters do not reach the experimentally observed AE. The calculated IE of one FA molecule is 11.4 eV. Adding water to the FA results in a general trend of lowering the IE values, as can be seen in Figure 4 Panel (B), the FA_1W_n series is demonstrated to converge to the experimental value of 10.5 eV (at the minimal IE). Panel (C) shows the obtained values for FA clusters with single water molecules. Here as well we observe a lowering of the IP as the number of FA molecules in the cluster increases. The experimental value of 10.5 eV is observed in the case of four and five FA molecules, whereas in the case of six or seven FA molecules, the minimal values are even lower, at 10.4 eV and 10.3 eV respectively. The fact that the experimental value is around 10.5 eV indicates that the observed clusters (at least the small ones) are likely a result of fragmentation from larger clusters.

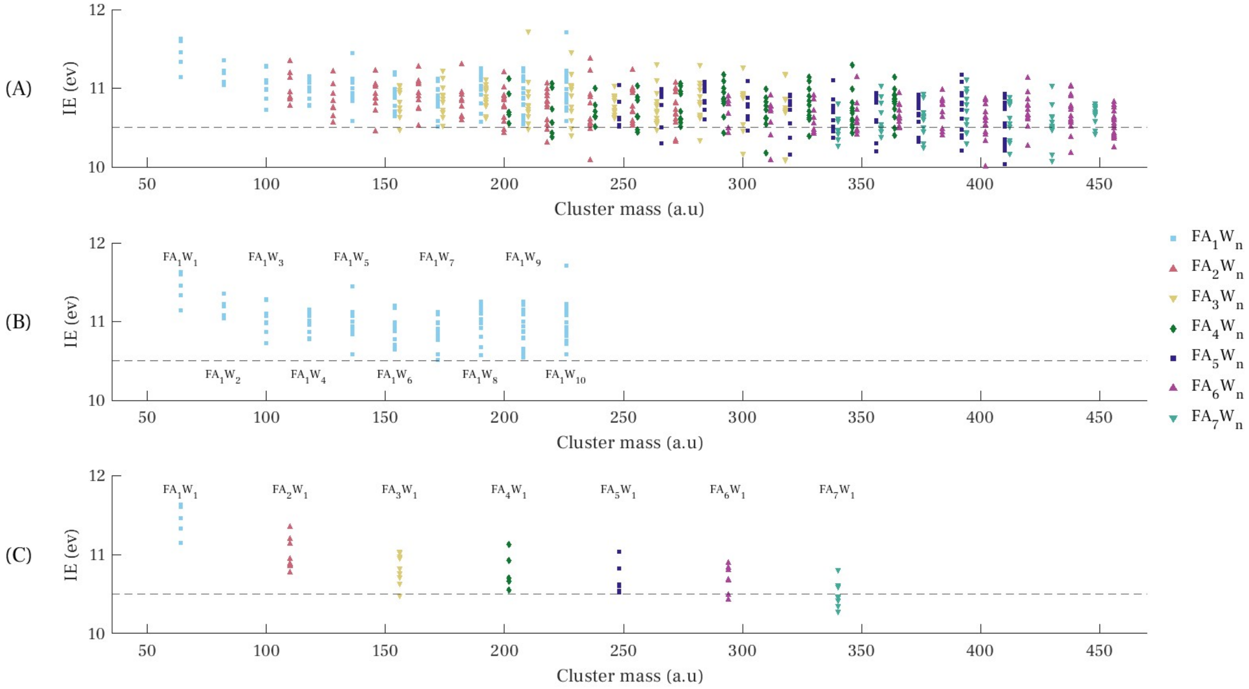

Figure 4: Ionization energies of different conformers of FA and water clusters at various sizes. Panel (A): IE of all calculated structures by cluster size. Colors represent the number of FA molecules in the cluster. Panel (B): direct comparison of IE for clusters composed of a single FA molecule with varying amounts of water molecules. Panel (C): IE of FA clusters of different sizes with a single water molecule

Conclusions

We have studied mixed FA water clusters using photoionization mass spectrometry coupled to tunable VUV radiation. Upon ionization, MS reveals protonated clusters of the form $FA_nW_mH^+$. Mass spectrometry reveals magic numbers for $FA_1W_5H^+$, $FA_2W_4H^+$, $FA_3W_3H^+$, $FA_4W_2H^+$, $FA_5W_1H^+$, $FA_6W_2H^+$ clusters, and shows that addition of water molecules to those structures results in structures with diminishing stability. nBE calculations demonstrate that the magic number clusters correspond to strongly bound clusters with large nBE values, characterized by a cyclic structure with molecules within the ring. The addition of water molecules interrupts the optimal arrangement and results in diminishing nBE. Experimental AE values converged to a value of 10.5 eV with only small effects from the cluster size and composition, calculated IE values indicate that those values correspond to larger clusters, thus indicating that the observed clusters are likely fragmented from larger ones.

Our theoretical results on photoionization dynamics in the formic acid water system will guide future experiments using ultrafast pump-probe spectroscopy being developed within our groups. We seek to measure the direct dynamics that occur between formic acid and water as the number of each moiety increases in the system. The interplay between FA and water particularly in the microscopic regime has also crucial bearings at the air-ice[5] and air-water interfaces,[50] and in catalytic chemistry.[5] We believe that these results will contribute to a better understanding of nucleation, cloud formation and chemistry that occurs on aqueous interfaces and aerosols by providing a molecular-level detail of how formic acid and water interact to form very stable clusters.

Acknowledgement

TS is grateful for the support from the Israel Science Foundation Grant No. 1941/20. MA, OK and AW are supported by the Gas Phase Chemical Physics Program, in the Chemical Sciences Geosciences and Biosciences Division of the Office of Basic Energy Sciences of the

U.S. Department of Energy under Contract No. DE-AC02-05CH11231 . This research used resources from the Advanced Light Source, which is a DOE Office of Science User Facility under Contract No. DE-AC02-05CH11231.

Supporting Information Available

Figures and coordinates of reported structures are available in the SI.

References

(1) Franco, B. et al. Ubiquitous atmospheric production of organic acids mediated by cloud droplets. *Nature* **2021**, *593*, 233–237.

(2) Woon, D. E. Quantum Chemical Cluster Studies of Cation–Ice Reactions for Astrochemical Applications: Seeking Experimental Confirmation. *Accounts of Chemical Research* **2021**, *54*, 490–497, PMID: 33444014.

(3) Martínez-Bachs, B.; Rimola, A. Gas-Phase vs. Grain-Surface Formation of Interstellar Complex Organic Molecules: A Comprehensive Quantum-Chemical Study. *International Journal of Molecular Sciences* **2023**, *24*.

(4) Wolf, M. E.; Turney, J. M.; Schaefer, H. F. High level ab initio investigation of the catalytic effect of water on formic acid decomposition and isomerization. *Phys. Chem. Chem. Phys.* **2020**, *22*, 25638–25651.

(5) Yang, P.; Liu, H.; Jin, Q.; Lai, Y.; Zeng, Y.; Zhang, C.; Dong, J.; Sun, W.; Guo, Q.; Cao, D.; Guo, J. Visualizing the Promoting Role of Interfacial Water in the Deprotonation of Formic Acid on Cu(111). *Journal of the American Chemical Society* **2024**, *146*, 210–217, PMID: 38037330.

(6) Rocha, W.; van Dishoeck, E.; Ressler, M.; van Gelder, M.; Slavicinska, K.; Brunken, N.; Linnartz, H.; Ray, T.; Beuther, H.; o Garatti, A. C.; others JWST Observations of Young protoStars (JOYS+): Detecting icy complex organic molecules and ions-I. CH4, SO2, HCOO-, OCN-, H2CO, HCOOH, CH3CH2OH, CH3CHO, CH3OCHO, and CH3COOH. *Astronomy & Astrophysics* **2024**, *683*, A124.

(7) Rodgers, S.; Charnley, S. Organic synthesis in the coma of Comet Hale-Bopp? *Monthly Notices of the Royal Astronomical Society* **2001**, *320*, L61–L64.

(8) Andrade, D. P.; de Barros, A. L.; Pilling, S.; Domaracka, A.; Rothard, H.; Boduch, P.; da Silveira, E. F. Chemical reactions induced in frozen formic acid by heavy ion cosmic rays. *Monthly Notices of the Royal Astronomical Society* **2013**, *430*, 787–796.

(9) Aviyente, V.; Zhang, R.; Varnali, T.; Lifshitz, C. Structures and energetics of proton-bound formic acid—water clusters,(HCOOH) n (H2O) H+. *International journal of mass spectrometry and ion processes* **1997**, *161*, 123–132.

(10) Zhang, R.; Wong, N.; Lee, S.; Zhu, R.; Han, K. Computation of large systems with an economic basis set: a density functional study on proton-bound carboxylic acid clusters. *Chemical Physics Letters* **2000**, *319*, 213–219.

(11) Velardez, G. F.; Ferrero, J. C.; Beswick, J. A.; Daudey, J. P. Ab initio study of the structures and $\pi^* \leftarrow$ n electronic transition in formic acid-(water) n (n= 3, 4, and 5) hydrogen bonded complexes. *The Journal of Physical Chemistry A* **2001**, *105*, 8769–8774.

(12) Aloisio, S.; Hintze, P. E.; Vaida, V. The hydration of formic acid. *The Journal of Physical Chemistry A* **2002**, *106*, 363–370.

(13) Baptista, L.; Andrade, D. P.; Rocha, A. B.; Rocco, M. L. M.; Boechat-Roberty, H. M.; da Silveira, E. F.; da Silva, E. C.; Arbilla, G. Theoretical investigation on the stability

of ionic formic acid clusters. *The Journal of Physical Chemistry A* **2008**, *112*, 13382–13392.

(14) Chen, H.-T.; Chang, J.-G.; Chen, H.-L. A Computational Study on the Decomposition of Formic Acid Catalyzed by (H2O) x, x= 0- 3: Comparison of the Gas-Phase and Aqueous-Phase Results. *The Journal of Physical Chemistry A* **2008**, *112*, 8093–8099.

(15) Nordstrom, C. M.; McGrath, A. J.; Thakkar, A. J. Microsolvation of the formic acid dimer—(HCOOH) 2 (H2O) n clusters with n= 1,..., 5. *Canadian Journal of Chemistry* **2010**, *88*, 736–743.

(16) Goken, E. G.; Joshi, K. L.; Russo Jr, M. F.; Van Duin, A. C.; Castleman Jr, A. Effect of formic acid addition on water cluster stability and structure. *The Journal of Physical Chemistry A* **2011**, *115*, 4657–4664.

(17) Inaba, S. Theoretical study of water cluster catalyzed decomposition of formic acid. *The Journal of Physical Chemistry A* **2014**, *118*, 3026–3038.

(18) Ivanov, S. D.; Grant, I. M.; Marx, D. Quantum free energy landscapes from ab initio path integral metadynamics: Double proton transfer in the formic acid dimer is concerted but not correlated. *The Journal of Chemical Physics* **2015**, *143*.

(19) Murdachaew, G.; Nathanson, G. M.; Gerber, R. B.; Halonen, L. Deprotonation of formic acid in collisions with a liquid water surface studied by molecular dynamics and metadynamics simulations. *Physical Chemistry Chemical Physics* **2016**, *18*, 29756–29770.

(20) Takahashi, O.; Yamanouchi, S.; Yamamoto, K.; Tabayashi, K. Theoretical study of the X-ray absorption spectra of small formic acid clusters. *Chemical physics letters* **2006**, *419*, 501–505.

(21) Thakkar, A. J. Small clusters of formic acid: Tests and applications of density functional theory with dispersion-correcting potentials. *Chemical Physics Letters* **2013**, *560*, 71–74.

(22) Tenorio, B. N. C.; Nascimento, M. A. C.; Rocha, A. B. Theoretical study of the absolute inner-shell photoionization cross sections of the formic acid and some of its hydrogen-bonded clusters. *The Journal of Chemical Physics* **2019**, *150*.

(23) Tachikawa, H. Proton transfer vs complex formation channels in ionized formic acid dimer: A direct ab initio molecular dynamics study. *The Journal of Physical Chemistry A* **2020**, *124*, 3048–3054.

(24) Maity, D. K. How much water is needed to ionize formic acid? *The Journal of Physical Chemistry A* **2013**, *117*, 8660–8670.

(25) Feng, W. Y.; Lifshitz, C. Evaporation of dimers from proton-bound formic acid clusters. *The Journal of Physical Chemistry* **1994**, *98*, 6075–6081.

(26) Goken, E.; Castleman Jr, A. Reactions of formic acid with protonated water clusters: Implications of cluster growth in the atmosphere. *Journal of Geophysical Research: Atmospheres* **2010**, *115*.

(27) Inokuchi, Y.; Nishi, N. Infrared photodissociation spectroscopy of protonated formic acid and acetic acid clusters. *The Journal of Physical Chemistry A* **2003**, *107*, 11319–11323.

(28) Inokuchi, Y.; Nishi, N. Infrared Photodissociation Spectroscopy of Protonated Formic Acid- Water Binary Clusters, H+·(HCOOH) n· H2O (n= 1- 5). Spectroscopic Study of Ion Core Switch Model and Magic Number. *The Journal of Physical Chemistry A* **2002**, *106*, 4529–4535.

(29) Heinbuch, S.; Dong, F.; Rocca, J.; Bernstein, E. Single photon ionization of hydrogen bonded clusters with a soft x-ray laser:(HCOOH) x and (HCOOH) y (H2O) z. *The Journal of chemical physics* **2007**, *126*.

(30) Li, K.; Ďurana, J.; Kocábková, B.; Pysanenko, A.; Yan, Y.; Ončák, M.; Fárník, M.; Lengyel, J. Hydrated Formic Acid Clusters and their Interaction with Electrons. *ChemPhysChem n/a*, e202400071.

(31) Cao, S.; Wu, X.; Chen, Y.; Qiu, S.; Liu, X.; Sun, C.; Piao, L. Water as a cocatalyst for photocatalytic H2 production from formic acid. *Nano Today* **2020**, *35*, 100968.

(32) Mahmoodi-Darian, M.; Lundberg, L.; Zöttl, S.; Scheier, P.; Echt, O. Electron attachment and electron ionization of formic acid clusters embedded in helium nanodroplets. *Journal of the American Society for Mass Spectrometry* **2019**, *30*, 787–795.

(33) Sutton, S. F.; Rotteger, C. H.; Jarman, C. K.; Tarakeshwar, P.; Sayres, S. G. Ultrafast Proton Transfer and Contact Ion-Pair Formation in Formic Acid Clusters. *The Journal of Physical Chemistry Letters* **2023**, *14*, 8306–8311, PMID: 37681673.

(34) Khuu, T.; Schleif, T.; Mohamed, A.; Mitra, S.; Johnson, M. A.; Valdiviezo, J.; Heindel, J. P.; Head-Gordon, T. Intra-cluster Charge Migration upon Hydration of Protonated Formic Acid Revealed by Anharmonic Analysis of Cold Ion Vibrational Spectra. *The Journal of Physical Chemistry A* **2023**, *127*, 7501–7509, PMID: 37669457.

(35) Pysanenko, A.; Gámez, F.; Fárníková, K.; Pluhařǒvá, E.; Fárník, M. Proton Transfer Reactions between Methanol and Formic Acid Deposited on Free Ar N Nanoparticles. *The Journal of Physical Chemistry A* **2019**, *123*, 7201–7209.

(36) Ahmed, M.; Kostko, O. From atoms to aerosols: probing clusters and nanoparticles with synchrotron based mass spectrometry and X-ray spectroscopy. *Phys. Chem. Chem. Phys.* **2020**, *22*, 2713–2737.

(37) Kostko, O.; Troy, T. P.; Bandyopadhyay, B.; Ahmed, M. Proton transfer in acetaldehyde–water clusters mediated by a single water molecule. *Phys. Chem. Chem. Phys.* **2016**, *18*, 25569–25573.

(38) Xu, B.; Stein, T.; Ablikim, U.; Jiang, L.; Hendrix, J.; Head-Gordon, M.; Ahmed, M. Probing solvation and reactivity in ionized polycyclic aromatic hydrocarbon–water clusters with photoionization mass spectrometry and electronic structure calculations. *Faraday Discuss.* **2019**, *217*, 414–433.

(39) Mackie, C. J.; Lu, W.; Liang, J.; Kostko, O.; Bandyopadhyay, B.; Gupta, I.; Ahmed, M.; Head-Gordon, M. Magic Numbers and Stabilities of Photoionized Water Clusters: Computational and Experimental Characterization of the Nanosolvated Hydronium Ion. *The Journal of Physical Chemistry A* **2023**, *127*, 5999–6011, PMID: 37441795.

(40) Wannenmacher, A.; Lu, W.; Amarasinghe, C.; Cerasoli, F.; Donadio, D.; Ahmed, M. An experimental and computational view of the photoionization of diol–water clusters. *The Journal of Chemical Physics* **2024**, *160*, 144303.

(41) Lu, W.; Mackie, C. J.; Xu, B.; Head-Gordon, M.; Ahmed, M. A Computational and Experimental View of Hydrogen Bonding in Glycerol Water Clusters. *The Journal of Physical Chemistry A* **2022**, *126*, 1701–1710, PMID: 35254809.

(42) Belau, L.; Wilson, K. R.; Leone, S. R.; Ahmed, M. Vacuum-Ultraviolet Photoionization Studies of the Microhydration of DNA Bases (Guanine, Cytosine, Adenine, and Thymine). *The Journal of Physical Chemistry A* **2007**, *111*, 7562–7568, PMID: 17419600.

(43) Belau, L.; Wilson, K. R.; Leone, S. R.; Ahmed, M. Vacuum Ultraviolet (VUV) Photoionization of Small Water Clusters. *The Journal of Physical Chemistry A* **2007**, *111*, 10075–10083, PMID: 17715907.

(44) Shao, Y.; Gan, Z.; Epifanovsky, E.; Gilbert, A. T.; Wormit, M.; Kussmann, J.; Lange, A. W.; Behn, A.; Deng, J.; Feng, X.; others Advances in molecular quantum chemistry contained in the Q-Chem 4 program package. *Molecular Physics* **2015**, *113*, 184–215.

(45) Mardirossian, N.; Head-Gordon, M. ωB97X-V: A 10-parameter, range-separated hybrid, generalized gradient approximation density functional with nonlocal correlation, designed by a survival-of-the-fittest strategy. *Physical Chemistry Chemical Physics* **2014**, *16*, 9904–9924.

(46) Kendall, R. A.; Dunning Jr, T. H.; Harrison, R. J. Electron affinities of the first-row atoms revisited. Systematic basis sets and wave functions. *The Journal of chemical physics* **1992**, *96*, 6796–6806.

(47) Martínez, L.; Andrade, R.; Birgin, E. G.; Martínez, J. M. PACKMOL: A package for building initial configurations for molecular dynamics simulations. *Journal of computational chemistry* **2009**, *30*, 2157–2164.

(48) Becke, A. D. A new mixing of Hartree Fock and local density functional theories. *The Journal of Chemical Physics* **1993**, *98*, 1372–1377.

(49) Nicolas, C.; Shu, J.; Peterka, D. S.; Hochlaf, M.; Poisson, L.; Leone, S. R.; Ahmed, M. Vacuum Ultraviolet Photoionization of C3. *Journal of the American Chemical Society* **2006**, *128*, 220–226, PMID: 16390150.

(50) de la Puente, M.; David, R.; Gomez, A.; Laage, D. Acids at the Edge: Why Nitric and Formic Acid Dissociations at Air–Water Interfaces Depend on Depth and on Interface Specific Area. *Journal of the American Chemical Society* **2022**, *144*, 10524–10529, PMID: 35658415.